OPTICAL PROCESS MODEL FOR LASER-ASSISTED TAPE WINDING

J.M. Reichardt[1,2], I. Baran[1,3], R. Akkerman[1,4]

[1]University of Twente, Faculty of Engineering Technology, The Netherlands
[2]Email: j.m.reichardt@student.utwente.nl
[3]Email: i.baran@utwente.nl
[4]Email: r.akkerman@utwente.nl

Keywords: tape winding, thermoplastic composites, optical properties, laser

Abstract
The present work is part of the EU-funded *ambliFibre* project in which a model-based on-line monitoring solution is being developed for the laser assisted tape winding (LATW) process of tubular fibre reinforced thermoplastic composite parts. Within this framework, an optical process simulation tool is developed using a ray tracing approach. A non-specular reflection model is implemented to model the anisotropic reflective behaviour of fibre-reinforced materials, using a bidirectional reflectance distribution function. The optical model is then coupled with a thermal model to predict the temperature distribution in the incoming tape and substrate during the LATW process. The proposed optical-thermal process model creates a link between the optical process parameters and the temperature evolution at the nip-point. Several optical parameters are investigated and it is found that the curvature and fibre orientation of the substrate are the most critical parameters that affect the nip-point temperature. The developed model is found to be relatively fast, yielding accurate results in a few seconds.

1. Introduction

The ongoing EU-funded *ambliFibre* project [1] aims to develop an intelligent model-based control system for laser-assisted tape winding (LATW) of fibre-reinforced thermoplastic (FRP) components. Within this framework, an optical process model is developed, which predicts the distribution of laser power on the tape and substrate (laminate).

Laser assisted tape winding (LATW) is an automated process to produce tubular or tube-like parts by winding a tape around a mandrel or liner. In this study, the material used is a unidirectionally reinforced thermoplastic material. During the process, the material is heated by a laser and pressure is applied by a roller, as is shown in Figure 1. The right process conditions (temperature and pressure) are needed to ensure good consolidation, with minimum amount of voids and good adhesion between layers.

Grouve [2] developed an optical-thermal model to predict the temperature of both tape and substrate. This model is relatively fast (a total computation time of 1.5 s is given) but limited to 2D. Stokes-Griffin and Compston [3] developed a far more detailed model in 3D, which includes the actual laser power distribution and requires a large (10 million, cf. 1000 for the former) number of rays. Both aforementioned optical models deal with flat substrates only.

Most of the previous efforts assumed that the composite material reflects light in a specular (mirror-like)

Excerpt from ISBN 978-3-00-053387-7

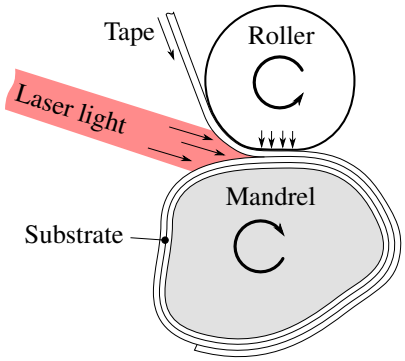

Figure 1. Schematic overview of the LATW process.

manner, although e.g. Grouve [2] notes that this does not match reality. Stokes-Griffin and Compston [3] attempted to improve on this by modelling the composite surface as a collection of *micro-half-cylinders* with a diameter of 10 µm. This approach, while yielding good results, requires a large number of rays in order to achieve convergence.

This paper presents an approach that improves on previous efforts by combining their advantages, in order to obtain an optical process model that is both fast and accurate. It includes the effects of laminate curvature, as well a non-specular reflection model based on a *bidirectional reflectance distribution function*. Any definition of the (non-uniform) laser power distribution and 3D geometry (machine and part) may be applied. The developed optical model is then coupled with a thermal model to predict the temperature distribution in the tape and substrate. The effects of optical parameters on the temperature are investigated using the proposed optical-thermal model.

The proposed optical model is planned to be part of a larger modelling "chain" as indicated in Figure 2(a), which covers all critical steps in the LATW process. Such a chain can be used for several purposes. The main objective is to include this model in a model-based system for on-line process control. Additionally, part production may be simulated in advance to assess the influence of process parameters and optimize their values. The structure of the optical-thermal model proposed here is shown in Figure 2(b), further details are given in the next section. Section 3 discusses the results obtained with the proposed model. An overview of conclusions, recommendations and planned future work concludes this paper.

2. Process model

A schematic view of the model structure is shown in Figure 2(b). The user provides a set of input parameters that are sent to the optical model, which is split in two main parts. The *macro-model* (section 2.1) launches a set of collimated rays from the (virtual) position of the laser. Then it calculates if and where this ray hits the geometry (tape, substrate or roller). The interactions between this ray and the tape and/or laminate are described by the *micro-model* (section 2.2), which describes the reflection and absorption at the material surface. Reflected light is modelled by spawning one or more new rays, which are sent back to the macro-model. This iterative process is terminated after a set number of reflections.

The output of the (combined) optical model is a two-dimensional laser irradiation field $q(\mathbf{x})$ that describes the heat flux (laser power per unit area) applied to the tape and the substrate. This information is used by a thermal model (section 2.3) to calculate the temperature. Because the focus of this paper is on the optical model, the temperature (of tape and substrate) is only calculated up to the nip-point, stopping just before the tape and substrate make physical contact.

Excerpt from ISBN 978-3-00-053387-7

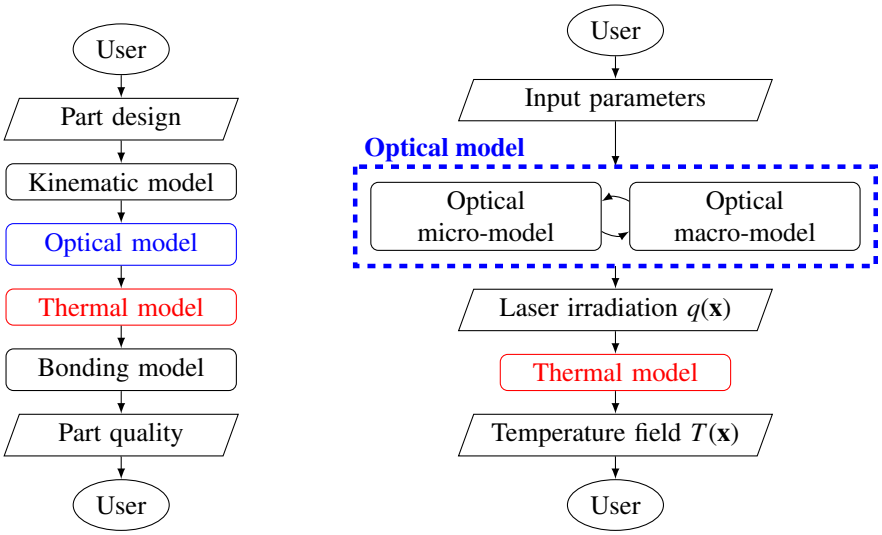

(a) Planned modelling approach (b) Structure of proposed optical-thermal model

Figure 2. Overview of LATW process model

2.1. Optical macro-model

The optical macro-model is designed to work with a geometry described by a triangle mesh. This formulation is completely generic, meaning that it is straightforward to include other geometric effects (e.g. roller deformation). The results presented here are obtained with the relatively simple geometry shown in Figure 3, with parameters listed in Table 1. The substrate is either singly curved with radius R_s or flat ($R_s \to \infty$). The curved surfaces are approximated using a finite number of triangular mesh elements, each spanning an angle of 5° (tape and roller) or 2° (substrate). *Phong normal-vector interpolation* [4] is used to ensure that the direction of the reflected light varies continuously, even though the curved surface is approximated by a set of flat segments.

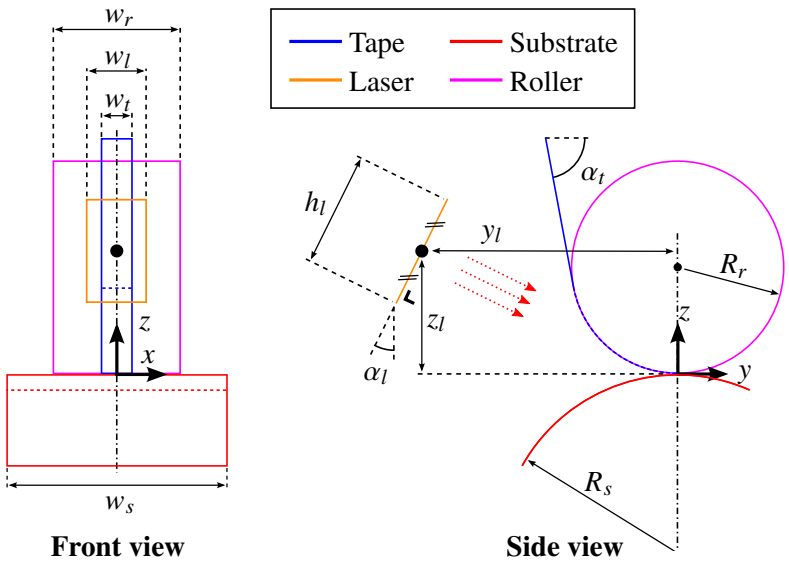

Figure 3. Model geometry used

Parameter	Value
Roller width, w_r	50 mm
Roller radius, R_r	34 mm
Laser spot width, w_l	12 mm
Laser spot height, h_l	30 mm
Laser angle, α_l	14°
Laser y-position, y_l	300 mm
Laser z-position, z_l	80 mm
Substrate width, w_s	50 mm
Substrate radius, R_s	*Varies*
Tape width, w_t	6 mm
Tape angle, α_t	90°

Table 1. Geometric parameters

Light hitting the roller is assumed to reflect specularly, with the reflectivity being a function of the angle of incidence according to the Fresnel equations. A roller with a polytetrafluoroethylene (PTFE) coating

Excerpt from ISBN 978-3-00-053387-7

is assumed, having a refractive index of $n_r = 1.4$ [5]. For the composite (tape and substrate), a more complicated micro-model described in section 2.2 is used. All non-reflected light is considered to be absorbed. The light absorbed by the tape and substrate is collected by square "bins" of 1 mm^2. The laser is modelled by launching N_0 light rays from the (virtual) laser position indicated in Figure 3. These rays are generated using Sobol sampling [6]. In this paper $N_0 = 16384$ is used, unless indicated otherwise.

2.2. Optical micro-model

The microscopic optical behaviour of the composite material is modelled using a *bidirectional reflectance distribution function* (BRDF), a concept first introduced in [7]. This BRDF is denoted as $\rho(\hat{\mathbf{k}}_i, \hat{\mathbf{k}}_r)$, i.e. it is a scalar function of the incoming light direction $\hat{\mathbf{k}}_i$ and the reflected light direction $\hat{\mathbf{k}}_r$, which are both unit vectors. Its definition may be understood by considering an incident light ray with energy Φ_i arriving from direction $\hat{\mathbf{k}}_i$, hitting a (macroscopic) surface patch δA with unit normal $\hat{\mathbf{n}}$, as is shown in Figure 4(a). Now the amount of energy reflected towards a small solid angle $\delta\Omega_r$ around direction $\hat{\mathbf{k}}_r$ is given by (Eq. 1). Integrating over the unit sphere[1] Ω yields the total reflected energy Φ_r (Eq. 2). The integral on the right-hand side should evaluate to at most unity (for all incident directions $\hat{\mathbf{k}}_i$) in order for energy to remain conserved, the remainder is considered to be absorbed.

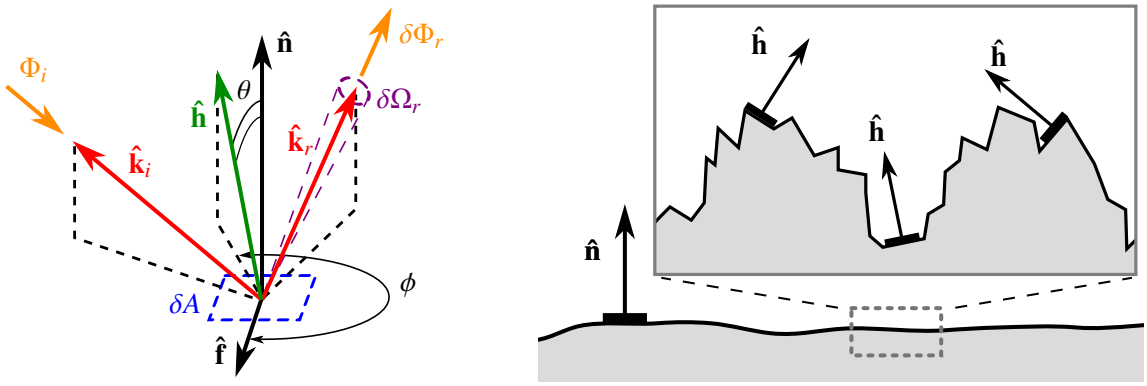

(a) Key BRDF-related quantities. The symbols are defined in the text.

(b) Surface (with macroscopic normal $\hat{\mathbf{n}}$) consisting of micro-facets with varying facet normal $\hat{\mathbf{h}}$

Figure 4. Illustration of the principles behind the BRDF

$$\delta\Phi_r = \rho(\hat{\mathbf{k}}_i, \hat{\mathbf{k}}_r)\,(\hat{\mathbf{k}}_r \cdot \hat{\mathbf{n}})\,\Phi_i\,\delta\Omega_r \tag{1}$$

$$\Phi_r = \Phi_i \int_\Omega \rho(\hat{\mathbf{k}}_i, \hat{\mathbf{k}}_r)\,(\hat{\mathbf{k}}_r \cdot \hat{\mathbf{n}})\,\mathrm{d}\Omega_r \tag{2}$$

In the present work a BRDF-formulation presented by Ashikhmin et al. [8] is implemented, which is based on microfacet theory. It defines the half-vector $\hat{\mathbf{h}}$ as the normalized mean of the incident and reflected directions ($\hat{\mathbf{k}}_i$ and $\hat{\mathbf{k}}_r$, respectively) as shown in Figure 4(a). The macroscopic surface is assumed to consist of a collection of small mirrors (microfacets) as shown in Figure 4(b), whose orientation can be described by a probability density function $p(\hat{\mathbf{h}})$.

The BRDF can then be expressed as given by (Eq. 3). In the numerator $p(\hat{\mathbf{h}})$ represents the aforementioned probability density function. $P(\hat{\mathbf{k}}_i, \hat{\mathbf{k}}_r, \hat{\mathbf{h}})$ is the *shadowing term* that represents the probability that a microfacet with orientation $\hat{\mathbf{h}}$ is visible from both directions $\hat{\mathbf{k}}_i$ and $\hat{\mathbf{k}}_r$. An expression for this was

[1] The BRDF used in this paper has the property that $\rho(\hat{\mathbf{k}}_i, \hat{\mathbf{k}}_r) = 0$ if $\hat{\mathbf{k}}_\mathbf{i} \cdot \hat{\mathbf{n}} \leq 0$ or $\hat{\mathbf{k}}_\mathbf{r} \cdot \hat{\mathbf{n}} \leq 0$, so integrating over the upper hemisphere is sufficient.

Excerpt from ISBN 978-3-00-053387-7

derived in [8], based on the assumption there is no significant correlation between the microfacet orientation and its position. Although this assumption may not be fully valid for a material which consists of cylinder-like fibres, it results in a relatively straightforward model that yields results similar to experimental observations [2, 3]. Finally, a Fresnel term $F(\hat{\mathbf{k}}_i \cdot \hat{\mathbf{h}})$ handles the microfacet reflectivity, while the terms in the denominator take care of normalization and geometric foreshortening.

$$\rho(\hat{\mathbf{k}}_i, \hat{\mathbf{k}}_r) = \frac{p(\hat{\mathbf{h}})\, P(\hat{\mathbf{k}}_i, \hat{\mathbf{k}}_r, \hat{\mathbf{h}})\, F(\hat{\mathbf{k}}_i \cdot \hat{\mathbf{h}})}{4C(\hat{\mathbf{k}}_i \cdot \hat{\mathbf{n}})(\hat{\mathbf{k}}_i \cdot \hat{\mathbf{n}})} \qquad \text{with } C = \int_\Omega p(\hat{\mathbf{h}})\, (\hat{\mathbf{n}} \cdot \hat{\mathbf{h}})\, \mathrm{d}\Omega_h \tag{3}$$

The microfacet distribution assumed here is an anisotropic Gaussian distribution (Eq. 4), with the angles θ and ϕ as indicated in Figure 4(a). Here the vector $\hat{\mathbf{f}}$ indicates the fibre orientation. The facet distribution is controlled by the standard deviations σ_f in fibre and σ_t in transverse direction. Unless mentioned otherwise, the values $\sigma_f = 0.05$ and $\sigma_t = 0.5$ are used, an example of the reflective behaviour obtained with these parameters is shown in Figure 5.

$$p(\hat{\mathbf{h}}) = \begin{cases} \exp\left(-\left(\dfrac{\cos^2\phi}{2\sigma_f^2} + \dfrac{\sin^2\phi}{2\sigma_t^2}\right)\tan^2\theta\right) & \text{if } \hat{\mathbf{h}} \cdot \hat{\mathbf{n}} > 0 \\ 0 & \text{if } \hat{\mathbf{h}} \cdot \hat{\mathbf{n}} \le 0 \end{cases} \qquad \text{with } \hat{\mathbf{h}} = (\sin\theta\cos\phi)\hat{\mathbf{f}} + (\sin\theta\sin\phi)\hat{\mathbf{t}} + (\cos\theta)\hat{\mathbf{n}} \tag{4}$$

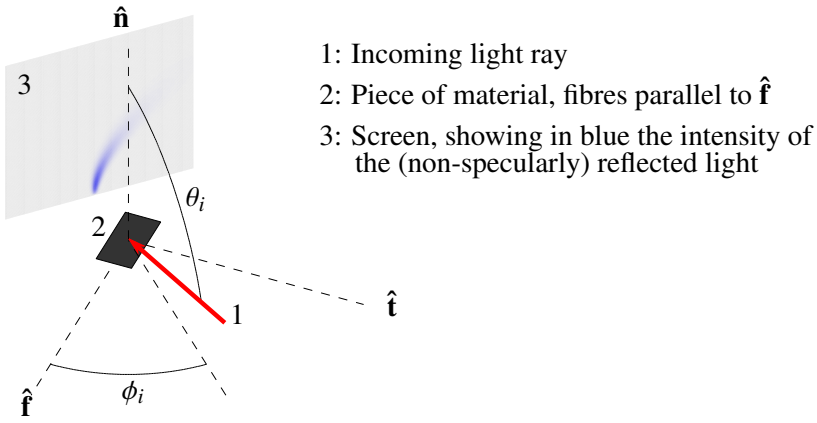

Figure 5. Example of reflective behaviour described by BRDF

Coupling the (continuous) BRDF with the macro-model based on (discrete) ray tracing is done as follows. The BRDF is first integrated over the hemisphere (Eq. 2) to determine the total reflected energy Φ_r, with the remainder being absorbed. A number of reflected rays $N_d = 5$ are then spawned, each carrying an amount of energy equal to Φ_r/N_d. The directions of these reflected rays are determined by considering the BRDF (or more accurately, (Eq. 1)) to be a probability distribution, from which the reflected directions are sampled randomly.

2.3. Thermal model

As aforementioned, the thermal model developed by Grouve [2] is coupled with the proposed optical model. The thermal properties are also taken from [2]. A collocation method is used to solve the 1D

Excerpt from ISBN 978-3-00-053387-7

heat equation in the through-thickness direction. This model uses a Lagrangian approach, calculating the temperature of a single piece of material as a function of time, with time and position (in the placement direction) related by the placement velocity $v = 100\,\mathrm{mm\,s^{-1}}$. A time-dependent heat flux (laser irradiation) is applied to both tape and substrate, which follows from the optical model. Convective and radiative losses to the surroundings are included. The relevant section of the (PTFE) roller is included with density $\rho = 2180\,\mathrm{kg\,m^{-3}}$, specific heat capacity $c_p = 1\,\mathrm{kJ\,kg^{-1}\,K^{-1}}$ and conductivity $k = 0.24\,\mathrm{W\,m^{-1}\,K^{-1}}$, assuming perfect contact between roller and tape. Effects of in-plane conduction are ignored, as well as tape or substrate curvature. The thermal model is run multiple times for various points in the width direction (x-direction, see Figure 3), because laser irradiation varies with this coordinate. A resolution of 1 mm is used in the width direction, the time step is $\Delta t = 0.05\,\mathrm{ms}$ unless mentioned otherwise.

3. Results

A "base case" is established using the model settings mentioned earlier, i.e. $N_0 = 16384$ initial rays and $N_d = 5$ reflected rays per incoming ray. The optical model is terminated after at most one iteration (reflection) and uses a flat substrate, which has a fibre orientation of 0° (i.e. fibres in the placement direction). All parameters related to the laser (having intensity $1217\,\mathrm{W\,mm^{-2}}$) are kept constant, because studying the obvious dependence of temperature on laser power (and distribution thereof) is not very useful at this stage. The optical model output (normalized irradiance) is shown in Figure 6(a). The thermal model uses this data to calculate the temperature field shown in Figure 6(b). The most critical results here are the averaged temperatures at the nip-point just prior to bonding, as indicated in Figure 6(b). In the case shown here, these are 322.1 °C for the tape and 115.1 °C for the substrate.

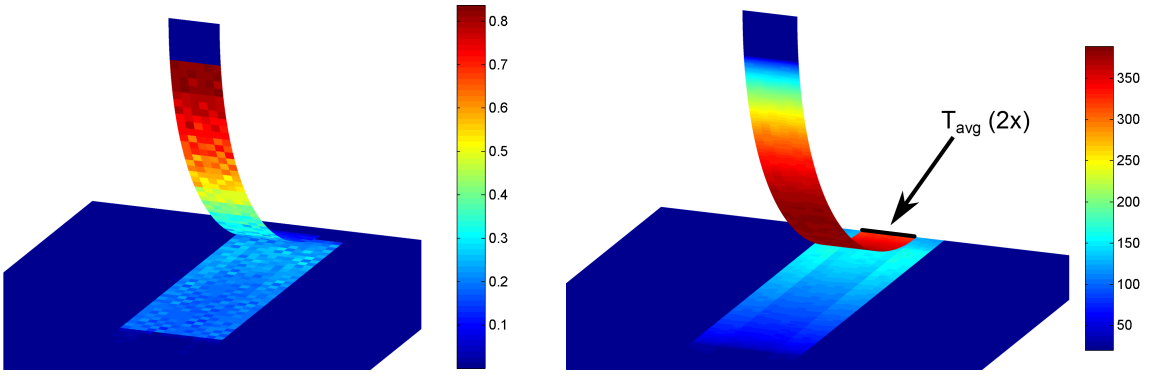

(a) Optical model output: normalized irradiance (b) Thermal model output: temperature field (°C)

Figure 6. Optical and thermal model results obtained with baseline settings

Figure 6 shows why it is necessary to assess the optical and thermal model in combination, instead of examining the optical model only. The optical model itself produces relatively noisy results, but the integrating behaviour of the thermal model smooths out this noise to a large extent. Trying to obtain near-perfect convergence of the optical model itself would thus result in a waste of computational resources.

Several parameters of the model are varied with respect to the base case, in order to assess which parameters have the most influence on the outcome (nip-point temperatures). Results are summarized in Table 2. Additionally, Figure 7 shows the nip-point temperatures for various radii of substrate curvature. A small radius increases the substrate temperature and decreases the tape temperature, because (due to the changing angle of incidence) more incoming light is absorbed by the substrate (so less is reflected).

Results from Table 2 provide insight into the influence of the optical micro-model. If the results with the BRDF-based optical micro model (#1) are compared to results in which simple specular (mirror-like)

Excerpt from ISBN 978-3-00-053387-7

#	Description	Tape temp. [°C]		Substrate temp. [°C]	
		Value	Difference	Value	Difference
1	**Base case**	322.1	-	115.1	-
2	Tape / substrate reflect specularly	324.0	1.9	126.5	11.4
3	Nearly-specular reflection ($\sigma_f = \sigma_t = 0.02$)	324.4	2.3	124.3	9.2
4	Substrate fibres at 45°	299.8	−22.3	130.5	15.4
5	Substrate fibres at 90°	295.3	−26.8	134.2	19.1
6	Substrate fibres at 90°, $\sigma_t = 0.25$ (was 0.5)	302.4	−19.7	131.8	16.7
7	Substrate fibres at 90°, $\sigma_f = 0.1$ (was 0.05)	297.9	−24.2	132.3	17.2
8	Tape refractive index $n_t = 1.9$ (was 1.8)	317.8	−4.3	116.0	0.9
9	Subs. refractive index $n_s = 1.9$ (was 1.8)	323.3	1.2	114.1	−1.0
10	$N_0 = 1024$ (was 16384), $N_d = 1$ (was 5), $\Delta t = 0.5$ ms (was 0.05 ms)	322.2	0.1	116.1	1.0
11	Include no reflections (direct light only)	274.6	−47.5	99.4	−15.7
12	Include at most 2 reflections (instead of 1)	324.3	2.2	121.9	6.8

Table 2. Results obtained with optical-thermal model for various parameters. The "Difference"-columns indicate the temperature differences with respect to the base case (#1)

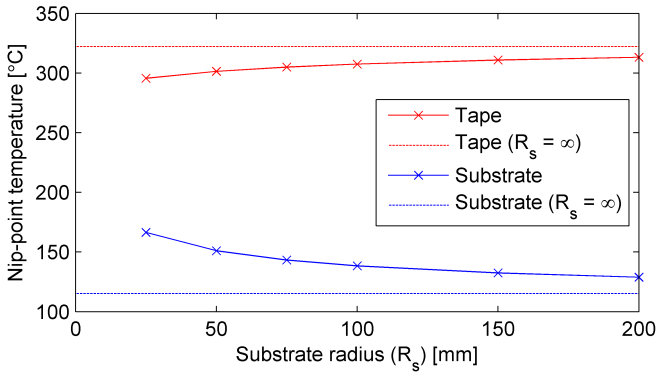

Figure 7. Nip-point temperatures as a function of substrate curvature

reflection is assumed (#2), the differences are relatively small. Note that a specular reflection model (#2) and a BRDF-based micro-model with a very "flat" microfacet distribution (#3) yield almost equal results. Larger differences appear when the substrate fibre orientation is 45° (#4) or 90° (#5). Absorption and substrate temperatures then increase, while less energy is reflected towards the tape.

The reflection micro-model contains several parameters that may be varied. The standard deviations σ_f and σ_t affect the assumed microfacet distribution and hence the shape of the reflection. Varying these parameters (#6 and #7) show that (compared to #5) the transverse parameter σ_t has the most influence. This is to be expected, as this parameter determines how much the light rays are "spread" in the direction transverse to the fibres. The refractive indices (#8 and #9, cf. #1) have comparatively little significance.

The simulation in the base case (#1) takes 93 s to execute in `MatLab` on a quad-core 2.4 GHz laptop, which does not vary significantly for the other cases considered so far (#2-#9). Drastically reducing the number of rays and increasing the time-step (Δt) of the thermal model (#10) reduces the execution time to around 11 s, more than half of which is needed to assemble the geometry, calculate normals and other "one-off" initialization tasks. The optical (micro and macro) model requires around 4 s in total. Including direct light only (#11) yields a speed-up but at an unacceptable loss of accuracy. Including one additional reflection (#12) on the other hand makes a relatively small difference, while increasing the time required to around 4.5 minutes.

Excerpt from ISBN 978-3-00-053387-7

4. Conclusions and future work

An optical model is developed that, coupled with a 1D thermal model, predicts the temperature evolution during the LATW process of thermoplastic composites, which is necessary for model based on-line process control. This model is used to assess the sensitivity of the LATW process to various parameters. Key parameters influencing the optical model are found to be the curvature and fibre orientation of the substrate. Relatively noisy optical results are found to be sufficient for the purposes of temperature prediction, as expected from the integrating behaviour of the thermal model. The developed model is found to be relatively fast, yielding accurate results in a few seconds.

Future work will focus on validating the developed model experimentally. Additional measurements may be needed to establish the required model parameters. In particular, experimental measurement of the reflective behaviour of the composite material will be required, to validate the optical micro-model and obtain values for its parameters. The optical model will be developed further to allow incorporation in a system for on-line process control, regulating laser power and distribution in real time.

Acknowledgments

This project has received funding from the European Union's Horizon 2020 research and innovation programme under grant agreement No 678875.

References

[1] European Commission. adaptive model-based control for laser-assisted fibre-reinforced tape winding, August 2015. [Online; accessed 12-April-2016].

[2] W. J. B. Grouve. *Weld strength of laser-assisted tape-placed thermoplastic composites*. PhD thesis, University of Twente, August 2012.

[3] C. M. Stokes-Griffin and P. Compston. A combined optical-thermal model for near-infrared laser heating of thermoplastic composites in an automated tape placement process. *Composites: Part A*, 75:104–115, 2015.

[4] Bui Tuong Phong. Illumination for computer generated pictures. *Commun. ACM*, 18(6):311–317, June 1975.

[5] R. H. French et al. Optical properties of materials for concentrator photovoltaic systems. In *Photovoltaic Specialists Conference (PVSC), 2009 34th IEEE*, pages 000394–000399, June 2009.

[6] I. M. Sobol. On the distribution of points in a cube and the approximate evaluation of integrals. *USSR Computational Mathematics and Mathematical Physics*, 7(4):86–112, 1967.

[7] Fred Nicodemus. Directional reflectance and emissivity of an opaque surface. *Applied Optics*, 4(7):767–775, 1965.

[8] Michael Ashikhmin, Simon Premože, and Peter Shirley. A microfacet-based brdf generator. In *Proceedings of the 27th Annual Conference on Computer Graphics and Interactive Techniques*, SIGGRAPH '00, pages 65–74, 2000.

Excerpt from ISBN 978-3-00-053387-7